

# Testing the Tube Super-Dielectric Material Hypothesis: Increased Energy Density Using NaCl

JONATHAN GANDY,<sup>1</sup> FRANCISCO JAVIER QUINTERO CORTES,<sup>2</sup>  
and JONATHAN PHILLIPS<sup>3,4</sup>

1.—Department of Mechanical and Aerospace Engineering, Naval Postgraduate School, 1 University Dr., Monterey, CA 93943, USA. 2.—Universidad Nacional de Colombia, Bogotá 111321, Colombia. 3.—Energy Academic Group, Naval Postgraduate School, 1 University Dr., Monterey, CA 93943, USA. 4.—e-mail: jphillip@nps.edu

The focus of the present work is the evaluation of the low-frequency dielectric performance of titanium dioxide nanotube arrays, created by anodization, filled with aqueous NaCl solutions. At low frequency (ca.  $<10^{-2}$  Hz), capacitors made up of this so-called tube super-dielectric material were found to have extreme dielectric constants, greater than 1 billion. The same capacitors also registered unprecedented energy densities, nearly  $400 \text{ J/cm}^3$ , better than that observed ( $<250 \text{ J/cm}^3$ ) for the same type of anodized titania filled with an aqueous solution of  $\text{NaNO}_3$ , and about an order of magnitude better than commercial supercapacitors. Sufficient data were collected to propose a correlation relating dielectric thickness and salt concentration to overall energy density.

**Key words:** Capacitors, titania, dielectric, super-dielectric material, NaCl

## INTRODUCTION

This research is a continuation of a program to evaluate the performance of capacitors based on a recently discovered/invented class of materials, super-dielectric materials (SDM).<sup>1–4</sup> These dielectric materials are made up of porous, electrically insulating solids in which the pores are filled with liquids containing ionic species (e.g., water with dissolved salt). The SDM hypothesis is that any porous dielectric material filled with a liquid phase containing ions in solution will have very high dielectric values, at least at low frequency, by virtue of the separation of ions/dipole formation in the liquid phase induced by an applied field.<sup>1,2</sup> The dipoles thus created in the dielectric will oppose the applied field, decreasing the net voltage, at any charge density on the electrodes, and concomitantly increasing the capacitance. In essence, the SDM hypothesis is an extension of the classical model of polarizable (or ponderable) materials.<sup>5</sup>

The first type of SDM studied, powder SDM (P-SDM), was fabricated by filling porous refractory oxide powders with aqueous solutions containing dissolved salt. High surface area oxide powders, for example alumina of the type used as supports in catalysis, were soaked to incipient wetness with water containing high concentrations of ions. These P-SDM were used to create electrostatic capacitors with dielectric constants, at low frequency, as high as  $10^{10}$ . For example, several alumina powders mixed and filled with salt (NaCl) water were found to have dielectric constants as much as seven orders of magnitude higher than that of the best dielectric, barium titanate.<sup>1,2,4</sup>

More recently, a second type of SDM, tube SDM (T-SDM), was built and tested.<sup>3</sup> These were transition metal oxide nanotube arrays, created by anodization of a metal foil substrate, and filled with aqueous salt solutions. In particular, titania was the first material tested as the oxide layer on anodized titanium seems particularly well suited to the creation of long dipoles. Titanium anodization produces hollow nanotubes, orthogonal to, and bonded to, the original metal surface.<sup>6–8</sup>

The purpose of the present study was to determine the impact of salt identity on the dielectric performance of T-SDM. In the first study of these materials, the liquid phase was an aqueous solution of  $\text{NaNO}_3$ . In the present case, similar T-SDM were created from anodized titania, as in the first study, but filled with an aqueous  $\text{NaCl}$  solution. The higher dielectric values and energy densities (ca.  $400 \text{ J/cm}^3$ ) observed for the  $\text{NaCl}$  solution supports the general SDM hypothesis that super-dielectrics are a large family of materials, and demonstrates that optimization (e.g., maximizing energy density) may require the variation of many parameters of construction of T-SDM.

## EXPERIMENTAL

### Anodization Process

Titanium foil, approx. 0.05 mm thick, was anodized to produce the electrodes using a well-known process.<sup>6–8</sup> The metal foils were anodized in a solution containing ammonium fluoride (0.25% w/w) and water (2.75% w/w) in ethylene glycol using a titanium cathode (2 cm from the anode). A constant direct current (DC) voltage of 40 V was applied for specific periods based on the desired tube length. The time was computed based on the observation that the titania tubes grow at a constant rate of approximately  $1 \mu\text{m}/25 \text{ min}$  in the bath employed. More detail is available elsewhere.<sup>3</sup> An example of the tubes formed is shown in Fig. 1. Clearly, the tubes, oriented with the long axis perpendicular to the surface of the parent foil, are organized in a regular, densely packed pattern.

### T-SDM Capacitor Assembly

For each capacitor, an anodized foil was submerged in an aqueous solution of  $\text{NaCl}$  (16.7 wt.% or 33.3 wt.%) for 50 min in order to fill the oxide nanotubes with the solution, constituting the super-dielectric material. One electrode was the titanium substrate underneath the nanotubes and the other was a rectangle of Grafoil (compressed natural graphite) of approximately  $1 \text{ cm}^2$  that nearly covered the entire anodized area. The circuit and the polarity of the capacitor were the same as described elsewhere.<sup>3</sup> The salt concentrations were designed to be (1) just below the known saturation value at 25 C ( $\sim 36\%$ ) such that no salt would precipitate, (2) half that value, and (3) no salt. The design concept was broad coverage of the impact of salt concentration.

### Charge/Discharge Protocol

Recent studies suggest that capacitance data for ferroelectric based capacitors is sometimes improperly extrapolated from ‘thick’ layer measurements without regard to saturation, maximum voltage, operating voltage and other factors,<sup>9</sup> leading to predicted energy densities for thin layers that far

exceed measured values. A second protocol that can also lead to over-predicted energy densities are measurements made at very low voltages, but extrapolated to predict behavior at high voltages. This difficulty may be inherent in the use of impedance spectroscopy, a method generally based on the determination of capacitance from measurements made at  $0 \pm 15 \text{ mV}$ .<sup>10–12</sup> In order to avoid these difficulties, very thin dielectric layers (ca.  $3 \mu\text{m}$ ) were chosen, and measurements of the resistor capacitor circuit (RC) time constants, using a load resistor measured to be  $10.8 \text{ k}\Omega$  in all cases, were made over far larger voltage ranges. In fact, using this approach, it was easy to demonstrate the dielectric constant changes as a function of voltage. The values of energy density and dielectric constant reported here are not extrapolations.

### Equivalent Circuit

Several of the capacitors were tested to determine the approximate values of  $R_{\text{int}}$  and  $R_{\text{out}}$  in the presumed equivalent circuit for the capacitor with an internal and output resistance, as discussed in detail elsewhere.<sup>3</sup>  $R_{\text{int}}$  is a measure of the internal resistance between the electrodes, and  $R_{\text{out}}$  is a measure of the internal capacitance resistance in series with the load resistor.  $R_{\text{out}}$  was determined by switching the load resistor ( $10.8 \text{ k}\Omega$ ) with a 10-M $\Omega$  multi-meter in voltage mode. This caused the voltage to jump up a small amount. On the basis of repeated readings, the output resistance was determined.  $R_{\text{int}}$  was determined simply by removing the load resistor, in the Region II voltage range (more in “Results”), and episodically, over hours, reading the remaining voltage. The value of  $R_{\text{int}}$  was then determined using an RC time constant computation.

## RESULTS

Only two parameters were varied in the study: the thickness of the titania layer and the concentration of  $\text{NaCl}$  in the ‘salt solution’ added to the anodized titania. Three capacitors (Table I) were filled with a low-salt (16.7 wt.%  $\text{NaCl}$ ) aqueous solution and five capacitors (Table II) with a high-salt (33.3 wt.%  $\text{NaCl}$ ) aqueous solution. The thickness of the dielectric (measured using SEM) ranged from  $3 \mu\text{m}$  to  $27 \mu\text{m}$ . Also, as a control, two films ( $3 \mu\text{m}$  and  $8 \mu\text{m}$ ) were filled with deionized water (no salt) and studied.

### Morphology

The anodized structures are nearly identical to those reported in an earlier study of T-SDM.<sup>3</sup> There are two features that ‘depart’ from the perfect tube model, and probably impact observed dielectric behavior. First, the top layer of the anodized material is covered with a relatively thin layer ( $< 1 \mu\text{m}$ ) of ‘grass’, or ‘very small tube’ titania oxide.

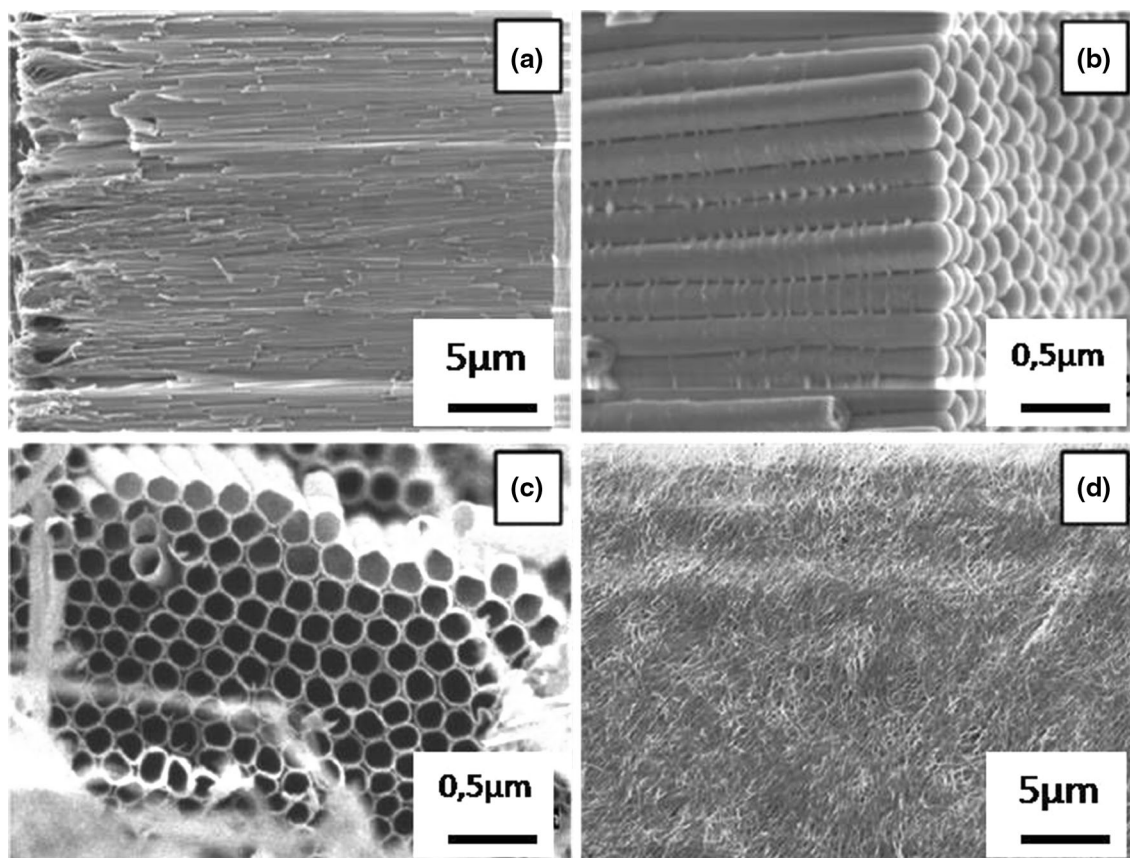


Fig. 1. SEM images of titania anodized for 4 h at 50 V. (a) Side view of 27- $\mu\text{m}$  tubes, including 'grass' layer. (b) Interface of tube array with metal surface, after removal (mechanical peel) from titanium foil. (c) Top of tube array after mechanical removal of  $\sim 1\text{-}\mu\text{m}$ -thick grass layer. (d) View of tube array from top prior to grass layer removal.

**Table I. Performance of capacitors (electrodes  $1\text{ cm}^2$ ) loaded with low-salt aqueous solutions**

TiO <sub>2</sub> layer thickness ( $\mu\text{m}$ )	Averaged energy density ( $\text{J}/\text{cm}^3$ )	% Energy, Region II	Capacitance, Region II (mF)	Dielectric constant, Region II
3	383	44	37	$1.30 \times 10^8$
8	334	77	199	$6.94 \times 10^8$
18	174	97	161	$3.41 \times 10^9$

**Table II. Performance of capacitors (electrodes  $1\text{ cm}^2$ ) loaded with high-salt aqueous solutions**

TiO <sub>2</sub> layer thickness ( $\mu\text{m}$ )	Averaged energy density ( $\text{J}/\text{cm}^3$ )	% Energy, Region II	Capacitance, Region II (mF)	Dielectric constant, Region II
3	233	79	51	$1.8 \times 10^9$
6	327	89	112	$7.93 \times 10^8$
8	396	89	192	$1.81 \times 10^9$
8	367	90	138	$1.3 \times 10^9$
18	166	93	151	$3.19 \times 10^9$
27	129	90	170	$5.4 \times 10^9$

The character of this layer, including its uniformity, is not consistent across an entire sample, and also not consistent between samples (Fig. 1d). Second, as the tubes get longer, they are less uniform and less

straight (Fig. 2), which noticeably impacts on tubes longer than  $\sim 15\ \mu\text{m}$ .

Thus, although at least 90% of the total length of the anodized layer for all tubes less than  $\sim 10\ \mu\text{m}$

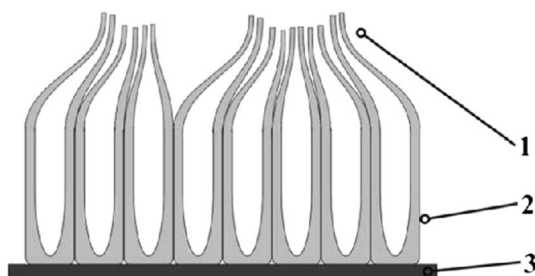


Fig. 2. Schematic of tube thinning for thicker titania layers. 1 Tubes become thinner, and tangled, near top for anodized layers  $>10 \mu\text{m}$  length. For tubes longer than  $\sim 10 \mu\text{m}$ , the top layer is so thin it appears as a form of ‘grass’ (Fig. 1d). 2 Straight, very regular, section of tubes, generally more than 90% of full length. 3 Tubes are closed at interface with underlying metal.

tall can be attributed to near-perfect tubes, thicker layers are clearly more complex and the impact of grassing and thinning more significant. The impact of these factors on the observed behavior is discussed in below.

### Discharge Behavior

Values for energy density, and dielectric constant were obtained from an average of at least three discharges (Fig. 3). The values of these parameters for the individual discharges never deviated more than  $\pm 20\%$  from the average value.

In this study, as in prior studies,<sup>1–4</sup> dielectric values were virtually constant in three regions of voltage. The lowest dielectric constants were found in Region I, between approximately 2.1 V and 1.8 V. In Region II, between approximately 1.8 V and 0.3 V, the dielectric values are far higher. The dielectric values found in Region III, less than 0.3 V, are the highest. For seven of the eight capacitors studied more than 75% of the energy was released in the Region II voltage region.

The basis for dividing the discharge into ‘regions’ is most easily observed on a plot of time versus  $\ln(V/V_0)$  (Fig. 4). A linear relationship corresponds to a constant dielectric/capacitance value, and the slope of each region is inversely proportional to the dielectric constant.

The energy density (Tables I and II) is computed by integration of voltage squared, divided by resistance (20 k $\Omega$ ) over the full discharge time. As outlined in the “Discussion”, the theory of T-SDM is that the energy density for a constant salt concentration should be independent of the tube length.

One objective of the present work was to test an earlier model of T-SDM energy density.<sup>3</sup> That model is based on the simple assumption that the dielectric constant of T-SDM is linearly proportional to dipole strength. In turn, dipole strength is clearly proportional to both the length of the pores, and the total salt in the aqueous phase. Thus, the T-SDM model predicts that energy density is independent of

pore length for any constant salt concentration in the aqueous solution (see “Discussion”).

In order to test the model, energy density as a function of tube length was determined (Fig. 5) for two different salt concentrations. Also shown is the predicted normalized energy density as a function of dielectric layer thickness for a constant dielectric constant material. In standard electrostatic theory, the energy density should be inversely proportional to the square of the distance between the electrodes. The data are clearly more consistent with the T-SDM model. Thus, it is reasonable to conclude that, for constant salt concentration, the ‘dielectric constant’ of T-SDM is approximately proportional to the square of the distance between the electrodes.

One result not entirely consistent with the T-SDM model is the non-linear relationship between salt concentration and measured dielectric constant. Specifically, although the two salt concentrations differed by a factor of two, there is no evidence of a relationship between salt concentration and dielectric value. A comparison of the dielectric values measured for the two salt concentrations (Table I versus Table II) shows no clear trend. The values for both salt concentrations vary more with thickness of the titania layer than they do with salt. A similar ‘non-correlation’ between salt concentration and energy density for T-SDM has been reported previously.<sup>3</sup> In contrast, for powder-SDM, there is a clear nearly linear relationship between salt concentration and dielectric constant.<sup>1,2,4</sup> One additional salient finding is that T-SDM filled with de-ionized water, no salt, have repeatedly been found in our laboratory, and elsewhere, to have dielectric constants of  $<100$ . Specifically, the measured discharge time (after lengthy ‘charging’) from  $\sim 2$  V to  $>0.1$  V was found to be of the order of 1 s for all salt-free controls.

### Equivalent Circuit

As described in the “Experimental” section, the values of input and output resistance for five of the capacitors was determined. Three main points emerge: (1) the output resistance (Table III) was consistently far below 1 k $\Omega$ ; (2) the internal resistance was at least 50 k $\Omega$  in all cases; and (3) thicker films had, surprisingly, lower resistance. As a point of comparison, the internal resistances are larger than those reported for many supercapacitors.

## DISCUSSION

### Overview

The capacitance data obtained in this study are best addressed from two perspectives. First, it should be addressed simply as novel observations that lead to remarkable comparisons with other types of capacitors. For example, it is clear that the energy density directly measured is the highest ever recorded. Second, the data should be understood as

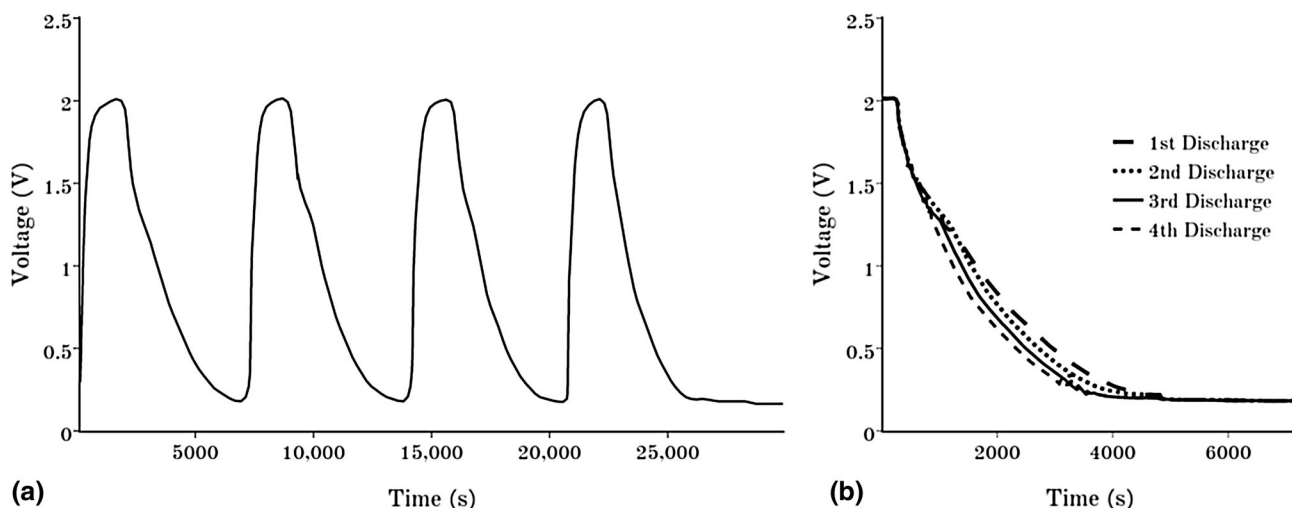


Fig. 3. Charge/discharge performance. (a) Cycles recorded for charging at 6 V, discharging through a 20-kΩ resistor. (b) Overlay of the four discharges.

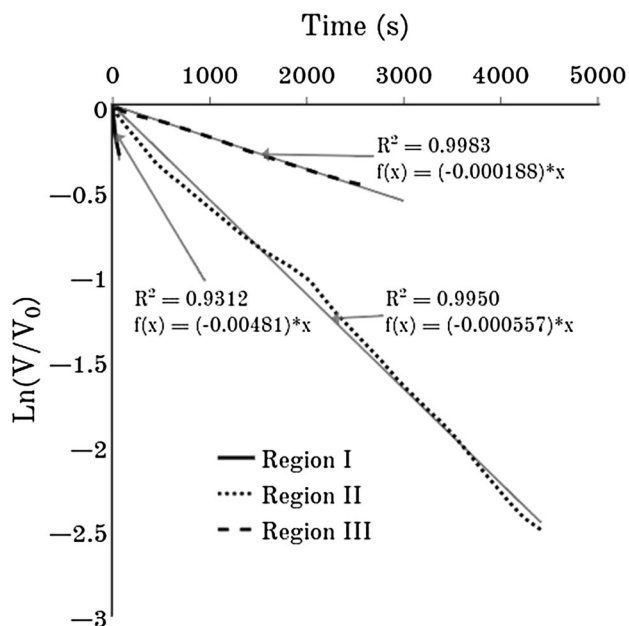


Fig. 4. Dielectric value versus voltage. Region I 2.1–1.8 V, Region II 1.8–0.3 V, Region III 0.3–0.1 V. These data are from the fourth cycle of Fig. 3.

yet another set of data consistent with the SDM hypothesis.

### Empirical Findings

On the level of direct measurement, several significant observations were made in the present study:

1. The volumetric energy density at low frequency of the capacitors studied in this paper are amongst the highest ever recorded (Table IV). The values obtained in this study are far higher

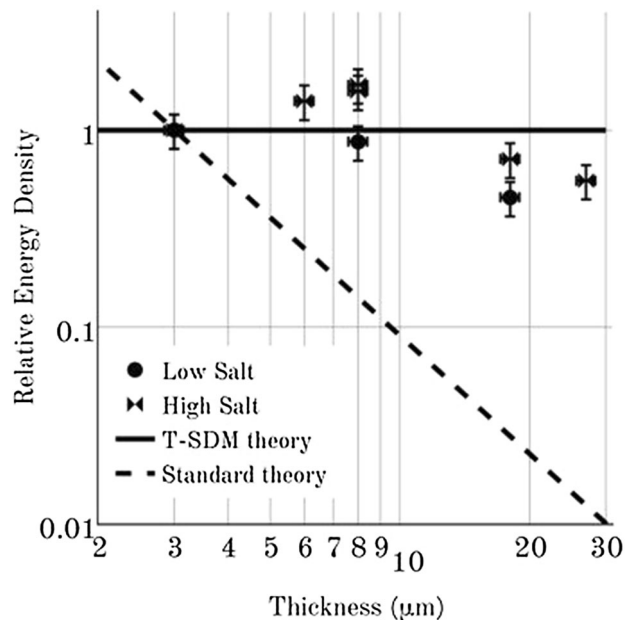


Fig. 5. Energy density versus distance between electrodes. Averaged normalized energy density data for each titania film thickness (Tables I and II). The energy densities were normalized by dividing the energy density by that measured for the 3-μm-thick samples. This was done independently for the high-salt (HS) and low-salt (LS) data (log-log). Standard theory (dashed line) indicates a drop in energy by a factor of 100 over a decade of thickness. TSDM theory predicts constant energy density for any salt concentration.

than those of other electrostatic capacitors, and nearly as high as the best prototype supercapacitor.

2. The energy density of capacitors studied is nearly independent of the thickness of the dielectric layer at constant salt concentration.
3. The measured dielectric constant values (Tables I and II) are clearly three to four orders

**Table III. Internal and output resistance values**

Anodized layer thickness (microns)	Low-salt $R_{int}$ (k $\Omega$ )	High-salt $R_{int}$ (k $\Omega$ )	Low-salt $R_{out}$ (k $\Omega$ )	High-salt $R_{out}$ (k $\Omega$ )
3	390	N.A.	0.3	N.A.
8	N.A.	140	N.A.	0.3
18	55	50	0.1	0.15
27	N.A.	60	N.A.	0.13

**Table IV. Recent advances in supercapacitors and electrostatic capacitors with high energy density**

Electrodes	J g <sup>-1</sup>	J cm <sup>-3</sup>	Refs.
Electrical double layer capacitors			
Porous carbon nanofiber	886	443 <sup>a</sup>	13
Graphene	457	324	14
Activated carbon from rice bran	252	115	15
Solid-state supercapacitor with carbon nanofibers	220	110 <sup>a</sup>	16
Nickel cobalt sulfide and carbon nanotubes	186	93 <sup>a</sup>	17
Copper–nickel oxide and activated carbon	181	90 <sup>a</sup>	18
Co <sub>3</sub> O <sub>4</sub> CoMoO <sub>4</sub> nanofoam	162	81 <sup>a</sup>	19
Dielectric material	J g <sup>-1</sup>	J cm <sup>-3</sup>	Refs.
Electrostatic capacitors			
Tube SDM with NaCl	120	390	This work
Tube SDM with NaNO <sub>3</sub>	70	230	3
Silica sol–gel coated by an organic acid	–	40	9
Polymer loaded with BaTiO <sub>3</sub> and TiO <sub>2</sub>	–	31.2	20
Polymer	–	27	21
Polymeric nanocomposite	–	17.5	22
Nanoporous anodic aluminum oxide with carbon nanotubes	7.2	–	23

<sup>a</sup>Volumetric energy density calculated assuming a bulk density of 0.5 g cm<sup>-3</sup> for carbonaceous electrodes.<sup>24</sup>

- of magnitude higher than ever claimed for solid dielectric materials, such as barium titanate,<sup>25–27</sup> colossal dielectric constant materials<sup>28–32</sup> and even polymer-derived dielectric materials. The values obtained are similar in magnitude, however, to earlier reported values for SDM, but significantly higher (nearly a factor of two) than NaNO<sub>3</sub>-loaded anodized titania.<sup>3</sup>
- Internal resistance values are larger than many reported for ‘supercapacitors’, and the output resistances lower.<sup>33,34</sup>
  - The variation of equivalent circuit internal resistance values as a function of salt concentration and anodized film thickness suggest measures can be taken to design T-SDM to meet requirements.

### T-SDM Model

The TSDM model is based on the simple assumption that the dielectric value is proportional to the reduction in field at the electrodes created by

induced dipoles in the dielectric material. In turn, this reduces the net voltage for any given charge on the electrodes. The reduction in field can be shown to be directly proportional to the effective dipole moment of the dielectric. This value is proportional to the product of dipole length and dipole ‘density’, the latter being a function of the free salt concentration. As developed in detail elsewhere,<sup>3</sup> this leads to the following simple expression for dielectric value as a function of dipole length energy, assuming constant dielectric structure and salt solution properties:

$$\text{Dielectric constant} \propto \frac{\text{Dipole Length} \times \text{Dipole Charge}}{\text{Dipole Density}} \quad (1)$$

Both length and total charge are proportional to tube length for a salt solution of constant salt concentration. The dipole density is proportional to the salt amount, which in turn is proportional to the tube length. Therefore, for a constant salt concentration:

$$\text{Dielectric constant} \propto (\text{Tube Length})^2 \quad (2)$$

Given this standard expression for energy density:

$$\begin{aligned} \text{Energy density} &= 1/2CV^2/\text{volume} \\ &= 1/2 \epsilon\epsilon_0 A/t/At = 1/2\epsilon\epsilon_0/t^2 \end{aligned} \quad (3)$$

Substituting Eq. 2 into Eq. 3, it is clear the energy density should be independent of the thickness of the dielectric layer.

A broad interpretation of the experimental data indicates the energy density (Fig. 5; Tables I and II) is nearly constant as a function of dielectric thickness. That is, relative to the standard expectation for dielectrics, a model which undoubtedly fits data for dielectric in which the dipole length is fixed, the measured drop in energy density ( $\sim 2$  times) with increasing thickness is minor compared to the predicted drop (81 times) over the full range of measured dielectric thickness ( $3\mu\text{m}$ – $27\mu\text{m}$ ). Examined in finer detail, the data do suggest that there is a modest decrease in energy density for dielectric thickness  $> \sim 10\mu\text{m}$ . This drop may reflect several, probably convoluted, parameters. First, the increased deviation of the physical structure from that of a system of perfectly formed tubes of constant diameter observed for anodized layer thicknesses greater than about  $10\mu\text{m}$ . As noted above, the tubes clearly become smaller in diameter and less straight above a length of about  $10\mu\text{m}$ s. Above about  $10\mu\text{m}$ , the top layer of the tubes loses mechanical strength and no longer stands upright. Instead, it falls across the top of the tube body. Given the variation in anodized film character, the possible difficulties with fully filling longer tubes with salt solution, and other irregularities associated with longer tubes, and considering an uncertainty of  $\pm 20\%$  in the actual capacitances arising from the differences from cycle to cycle and a conservative  $\pm 5\%$  for the measured tube lengths, the data are consistent with the TSDM model (Eq. 2).

A second parameter, reduction in internal resistance with increased tube length, might also explain part of the observed drop in energy density with tube length. For example, assuming a simple voltage divider model, the fraction of energy ‘dropped’ across  $R_{\text{int}}$ , relative to that dropped across the load resistor is a function of the ratio of the load resistance to the internal resistance. As an example, if the internal resistance of the high-salt sample/ $18\mu\text{m}$  sample was the same as that for the high-salt/ $8\mu\text{m}$  sample, the energy drop over the load for the  $18\mu\text{m}$  tube would have been larger than that observed ( $166\text{ J/cm}^3$ ), in fact close to  $\sim 190\text{ J/cm}^3$ . Change in internal resistance does not explain all observed drop in energy density with tube length, but it explains part. Moreover, the source of the reduced internal resistance might also be related to

morphological changes in the tubes with increased length. For example, longer tubes may be weaker and more likely to break/crack during capacitor construction, concomitantly creating lower resistance paths between electrodes.

There are no alternative models of high dielectric values/capacitance in the literature consistent with the observations reported. This statement is considered relative to some standard models of high capacitance. First, a standard supercapacitor model is not appropriate. High capacitance in standard capacitors is only reported in systems with no salt, a result completely consistent with the theory of supercapacitors,<sup>33,35</sup> but completely at odds with the results reported above. Moreover, supercapacitors require high surface area, electrically conductive, solid, electrode material, generally a form of carbon. A high surface area, solid, electrically conductive material is nowhere to be found in a T-SDM. Next, simple arguments also indicate the concept of colossal dielectric<sup>28–32</sup> behavior does not apply. Indeed, why would the introduction of salt into the liquid phase of a T-SDM increase the density of ‘surface states’? In the absence of liquid, the titania nanotube arrays have very, very low dielectric values. Hence, if there are ‘surface states’, that somehow lead to colossal dielectric values, they must be associated with the liquid. Does it even make sense to discuss ‘surface states’ vis-à-vis liquids? And what is the roll of salt? Other models of high dielectric values include the impact of metal particles<sup>36–38</sup> and the impact of creating a dielectric material at the percolation limit.<sup>39–41</sup> There are no metal particles in the T-SDM, and there is no reason to believe that there is some phase in the T-SDM near a percolation limit.<sup>42</sup>

Thus, these final, rather restricted, conclusions are reached regarding models: (1) the present data are fully consistent with the T-SDM model, and (2) there are no other models of high energy density capacitors that explain all of the observations made here and in previous reports of T-SDM.

Another consideration is the impact of equivalent circuit parameters on measured values. For example, given that the ‘internal resistance’ and the load resistance form a voltage divider circuit, the measured capacitance values in all cases are minima. That is, given an infinite internal resistance, all the current would pass through the load, and this would yield a higher effective capacitance than those measured.

Trends in internal resistance with parameters suggest design ‘dials’ for different applications. Long-term storage of charge would be more effective at lower salt concentrations, which apparently have a higher internal resistance. Possibly, higher salt concentration would be an advantage for rapid delivery of power. The purpose of the present study was to scout issues. It is clearly established that complete and quantitative understanding is a task bigger than a single study.

A final issue is the impact of the total number of ions in solution. In the earlier work, sodium nitrate was employed, whereas in the present case it was sodium chloride, both near saturation concentrations. At room temperature, the former has approximately 1.8 times more moles, and presumably ions, in aqueous solution at saturation, yet it is solutions of the latter which produced the higher dielectric and energy density values. This is puzzling given the proposed model, and indicates that the impact of salt on behavior of T-SDM, as well as aspects of the theory, are subjects for further study.

## REFERENCES

1. S. Fromille and J. Phillips, *Materials* 7, 8197 (2014).
2. F.J.Q. Cortes and J. Phillips, *J. Electron. Mater.* 44, 1367 (2015).
3. F.J.Q. Cortes and J. Phillips, *Materials* 8, 6208 (2015).
4. N.J. Jenkins, C. Petty, and J. Phillips, *Materials* 9, 118 (2016).
5. J.D. Jackson and L.C. Levitt, *Phys. Today* 15, 62 (1962).
6. V. Zwilling, E. Darque-Ceretti, A. Boutry-Forveille, D. David, M.Y. Perrin, and M. Aucouturier, *Surf. Interface Anal.* 27, 629 (1999).
7. P. Roy, S. Berger, and P. Schmuki, *Angew. Chem. Int. Ed.* 50, 2904 (2011).
8. F.J.Q. Cortes, P.J. Arias-Monje, J. Phillips, and H. Zea, *Mater. Des.* 96, 80 (2016).
9. Y. Kim, M. Kathaperumal, V.W. Chen, Y. Park, C. Fuentes-Hernandez, M.-J. Pan, B. Kippelen, and J.W. Perry, *Adv. Energy Mater.* (2015). doi:10.1002/aenm.201500767.
10. E. Barsoukov and J. Ross Macdonald, *Impedance Spectroscopy: Theory, Experiment, and Applications* (Hoboken: Wiley, 2005).
11. J. Ross Macdonald and W.R. Kenan, *Impedance Spectroscopy: Emphasizing Solid Materials and Systems* (Hoboken: Wiley, 1987).
12. C. Pazde-Araujo, R. Ramesh, and G.W. Taylor, *Science and Technology of Integrated Ferroelectrics: Selected Papers from Eleven Years of the Proceedings of the International Symposium of Integrated Ferroelectronics*. (Boca Raton, CRC Press, 2001).
13. C.H. Kim, J.-H. Wee, Y.A. Kim, K.S. Yang, and C.-M. Yang, *J. Mater. Chem. A Mater. Energy Sustain.* 4, 4763 (2016).
14. Y. Xu, Z. Lin, X. Zhong, X. Huang, N.O. Weiss, Y. Huang, and X. Duan, *Nat. Commun.* 5, 4554 (2014).
15. J. Hou, C. Cao, X. Ma, F. Idrees, B. Xu, X. Hao, and W. Lin, *Sci. Rep.* 4, 7260 (2014).
16. D.W. Lawrence, C. Tran, A.T. Mallajoyula, S.K. Doorn, A. Mohite, G. Gupta, and V. Kalra, *J. Mater. Chem. A Mater. Energy Sustain.* 4, 160 (2016).
17. P. Wen, M. Fan, D. Yang, Y. Wang, H. Cheng, and J. Wang, *J. Power Sources* 320, 28 (2016).
18. R. Li, Z. Lin, X. Ba, Y. Li, R. Ding, and J. Liu, *Nanoscale Horiz.* 1, 150 (2016).
19. J. Wang, X. Zhang, Q. Wei, H. Lv, Y. Tian, Z. Tong, X. Liu, J. Hao, H. Qu, J. Zhao, Y. Li, and L. Mai, *Nano Energy* 19, 222 (2016).
20. X. Zhang, Y. Shen, B. Xu, Q. Zhang, L. Gu, J. Jiang, J. Ma, Y. Lin, and C.-W. Nan, *Adv. Mater.* 28, 2055 (2016).
21. O.L. Smith, Y. Kim, M. Kathaperumal, M.R. Gadinski, M.-J. Pan, Q. Wang, and J.W. Perry, *ACS Appl. Mater. Interfaces* 6, 9584 (2014).
22. Y. Chen, X. Tang, J. Shu, X. Wang, W. Hu, Q.-D. Shen, *J. Polym. Sci. B.* 54, 1160 (2016).
23. F. Han, G. Meng, F. Zhou, L. Song, X. Li, X. Hu, X. Zhu, B. Wu, and B. Wei, *Sci. Adv.* 1, e1500605 (2015).
24. S. Murali, N. Quarles, L.L. Zhang, J.R. Potts, Z. Tanb, Y. Lub, Y. Zhub, and R.S. Ruoffa, *Nano Energy* 2, 764–768 (2013).
25. K. Kinoshita and A. Yamaji, *J. Appl. Phys.* 47, 371 (1976).
26. G. Arlt, D. Hennings, and G. de With, *J. Appl. Phys.* 58, 1619 (1985).
27. J.C. Burfoot and G.W. Taylor, *Polar Dielectrics and Their Applications* (Berkeley: University of California Press, 1979).
28. P. Lunkenheimer, S. Krohns, S. Riegg, S.G. Ebbinghaus, A. Reller, and A. Loidl, *Eur. Phys. J.* 180, 61 (2009).
29. P. Lunkenheimer, V. Bobnar, A.V. Pronin, A.I. Ritus, A.A. Volkov, and A. Loidl, *Phys. Rev. B* 66, 052105 (2002).
30. P. Lunkenheimer, R. Fichtl, S.G. Ebbinghaus, and A. Loidl, *Phys. Rev. B* 70, 172102 (2004).
31. S. Krohns, J. Lu, P. Lunkenheimer, V. Brize, C. Autret-Lambert, M. Gervais, F. Gervais, F. Bouree, F. Porcher, and A. Loidl, *Eur. Phys. J. B* 72, 173 (2009).
32. Ch Kant, T. Rudolf, F. Mayr, S. Krohns, P. Lunkenheimer, S.G. Ebbinghaus, and A. Loidl, *Phys. Rev. B* 77, 045131 (2008).
33. B.E. Conway, *Electrochemical Supercapacitors: Scientific Fundamentals and Technological Applications* (New York: Springer, 2013).
34. H. Gualous, D. Bouquain, A. Berthian, and J.M. Kauffmann, *J. Power Sources* 123, 86 (2003).
35. F. Beguin and E. Frackowiak, *Supercapacitors: Materials, Systems and Applications* (Weinheim: Wiley-VCH, 2013).
36. C. Pecharroman, F. Esteban-Betegon, F. Bartolome, J.F. Lopez-Esteban, and J. Moya, *Adv. Mat.* 13, 1541 (2001).
37. C. Pecharroman, F. Esteban-Betegon, and R. Jimenez, *Ferroelectrics* 400, 81 (2010).
38. S.K. Saha, *Phys. Rev. B* 69, 125416 (2004).
39. D.J. Bergman and Y. Imry, *Phys. Rev. Lett.* 39, 1222 (1977).
40. A.L. Efros and B.I. Shklovskii, *Phys. Stat. Sol. B* 76, 475 (1976).
41. A.L. Efros, *Phys. Rev. B* 84, 155134 (2011).
42. D. Gerenrot, L. Berlyand, and J. Phillips, *IEEE Trans. Adv. Packag.* 26, 410 (2003).